Journal of Medical Imaging and Health Informatics
Vol. 1, 284–289, 2011

Force Control of Intelligent Laparoscopic Forceps

Soheil Kianzad, Soheil O. Karkouti, and Hamid D. Taghirad*

Advanced Robotics and Automated Systems (ARAS), Department of Systems and Control, Faculty of Electrical and Computer Engineering, K. N. Toosi University of Technology, P.O. Box 16315-1355, Tehran, Iran

Actuators play an important role at the end-effectors of Minimally Invasive Surgery (MIS) robots. Having local, lightweight and powerful actuators would increase dexterity of surgeons. Shape Memory Alloy (SMA) actuators are considered as good candidates and presented significant behaviors in producing the force needed for grasping. Most of the current MIS systems provide surgeons with visual feedback. However, in many operations this information could not help surgeons to diagnose the manipulated tissue accurately. Therefore, having force and tactile information is also necessary. In order to have this information, local sensors are needed to give force feedback. This would also help to have control over the wire tension and prevent exceeding force causing tissue damages. In this paper a novel design of forceps that uses antagonistic SMA actuators is presented. This configuration helps to increase force and speed and also eliminates the bias spring used in similar works. Moreover, this antagonistic design makes it possible to place the force sensors at the back part of the forceps instead of attaching them to the jaws which results in a smaller forceps design. To control the exerted force, analytical model of system and a force control method are also presented. This enhanced design seems to address some of the existing shortcomings of similar models and remove them effectively.

Keywords: Antagonistic, Force Control, Force Feedback, Minimal Invasive Surgery, Shape Memory Alloys.

1. INTRODUCTION

Minimally Invasive Surgery (MIS) is a progressive field of study that attracts interests from many researchers.[1–3] This surgical method provided patients with several benefits such as less pain, short hospital stay, reduction of infection and recovery period.[2] Since their introduction to surgical world, medical robots had undergone a lot of innovation in terms of helping surgeons to have safe, quick and easy surgery.[3] These efforts resulted in telemanipulation robots that are now commercially available. With these robots such as da-Vinci, surgeon's hand movements can be scaled, filtered and seamlessly transferred into precise movements of end-effectors.[4] Among five essential parts of each medical robot (controller, arm, drive, end-effectors and sensors) end-effectors are considered as one of the important parts of manipulator design since they should have a good performance in patient's body through a small incision. Actuators play an important role in designing of the end-effectors. Among all available actuators, piezoelectric, SMA and dc micro-motors are the most common ones being used.[1,3,5] Kornbluh et al. have compared piezoelectric and SMA actuators and showed that both of them could provide high stress. But the strain rate for piezoelectric actuators is much lower than shape memory alloys, resulting in a lower stroke compared to SMA.[6] However, it is generally believed that shape memory alloy actuators are slow,[1] but their cycle speed could significantly be increased using short high current pulses and water cooling.[7] DC micro-motors have a good speed and large strain, but they have a low output torque.[1]

Considering the characteristics mentioned for actuators, it can be seen that almost all of them have some drawbacks, despite their various positive aspects. This has led several recent works to combine different actuators in order to achieve better performance. However, these hybrid configurations have also their own shortcomings. Kode and Cavusoglu[1] have used a DC motor and SMA wires in their actuator design, but since SMA wires cannot produce a forward-direction force to return the jaws to their default position, this necessitated to design a pre-loading spring. One of the main disadvantages of these bias-type SMA actuator configurations is their lack of active control for movement.[8]

On the other hand, there are some reports and evidences indicating injuries caused by laparoscopic surgery which have raised doubts about its efficiency versus conventional surgical methods. These doubts lead to this question: Are the forces applied by the tools in this method the same as those in conventional surgical ones?[9] In order to answer this question, it is necessary to have information about generated forces. Placing sensors for measuring these forces and their wirings appear to be hard as the tools become smaller in size.[10] However, this lack of force feedback and sensation in small tools cannot be neglected easily.

Moreover, although visual feedback provided in conventional MIS systems gives the surgeon many information about the manipulated tissue, this visual perception is not sufficient enough

*Author to whom correspondence should be addressed.

 2156-7018/2011/1/284/006 doi:10.1166/jmihi.2011.1042

for dexterous surgical procedures.[11] In other words, necessity of having force feedback can be determined in two parts:
(1) Surgeons need tactile and kinesthetic information and visible information together to properly diagnose details of the tissue being manipulated.[5, 10]
(2) Excessive mechanical stress may cause injury in tissues during grasping for elevation, exposure or manipulation.[12]

In this paper, a novel design of forceps using antagonistic shape memory alloy configuration is presented to overcome the shortcomings mentioned for MIS tools. This design facilitates sensor placement and thus provides surgeons with information about the exerted force. Increased force and speed and a smaller design are the other positive aspects of this configuration. Exact modeling of system and a control method are also presented in order to manipulate the applied force and improve the response of the system. This intelligent configuration helps surgeons to have information about the mechanical impedance of the tissue, in order to diagnose the tissue more accurately. Using the force feedback provided in this design, tissue damages due to excessive forces will certainly decrease. This can also be achieved by obtaining stress-length ratio curve of the tissues, in order for the surgeon to be able to apply the required force for grasping at different positions.

The rest of the paper is organized as follows. Section 2 presents the antagonistic actuator configuration and sensor placement. In Section 3 analytical modeling of the system and the proposed control method are described. Conducted experiments and the results obtained from system are presented in Section 4. Finally, Section 5 concludes the paper.

2. EXPERIMENTAL SETUP AND DESIGN

2.1. Actuator Part

The antagonistic actuator design consists of two sets of SMA wires: one set for opening the jaws, and another set for closing them. Since having more wires helps to produce greater forces, each set has several SMA wires; therefore, different force gains can be obtained both by changing the number of active SMA in each set and their input voltages. The SMA wires used in this design are 381 μm-diameter Flexinol[a].

Due to the fact that the force needed for closing the jaws (holding a tissue) is greater than the one needed for opening them, by placing different number of wires on each set, it is possible to have different forces for opening and closing the jaws. In this design, two SMA wires were used for closing and one wire for opening the jaws. A small pulley changes the direction of lower set of SMA. As shown in Figure 1(d), two forces are exerted by the jaws. Each of these forces could be defined as a function of the applied force to the upper rod, F and θ, the angle between the jaws of the grasper. θ itself is related to the position of the upper rod. In Fig. 1(d), let x be the position of the rod. Basic trigonometric mathematics yields

$$\theta = \tan^{-1}\left(\frac{y}{x+\Delta x}\right) \quad (1)$$

Note that y is the distance of the center of two rods from each other and is constant.

[a]Flexinol is a trademark of Dynalloy, Inc.

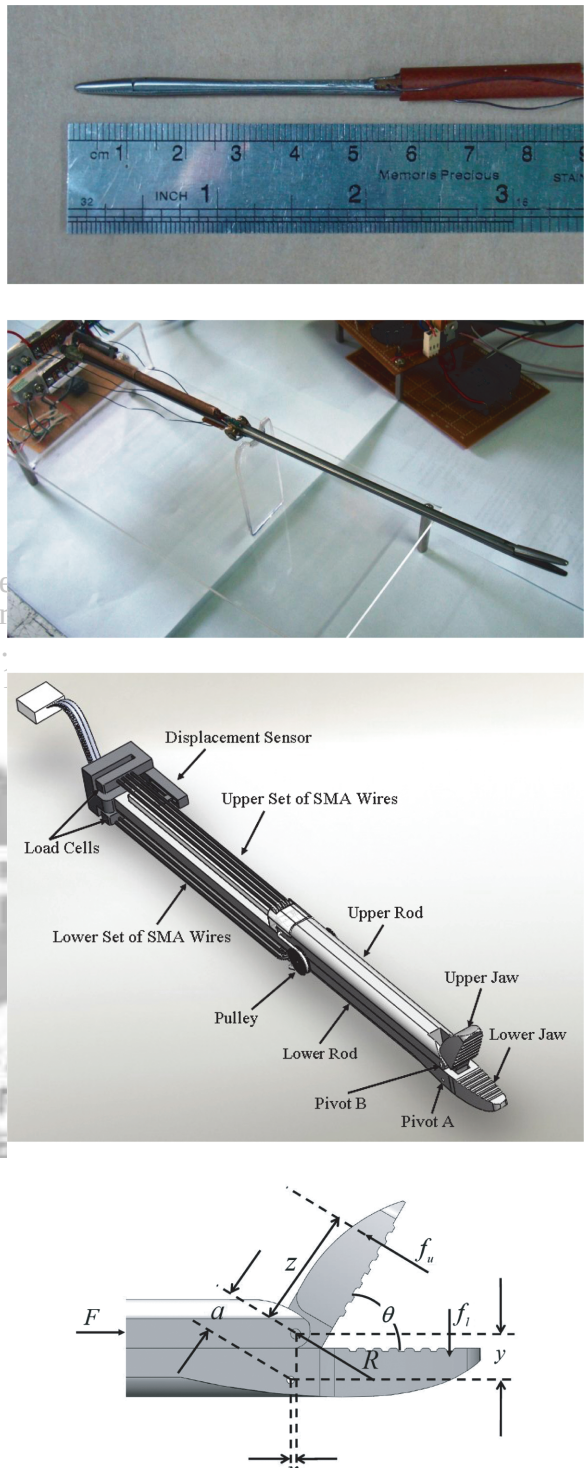

Fig. 1. Configuration of the intelligent forceps. (a) Photograph of the minimal grasper. (b) Photograph of the experimental setup. (c) Upper set of SMA wires activated. (d) Detailed view of the tool tip.

Considering the fact that the acceleration toward x axis is zero, Newton's second law can be written as

$$\sum F_x = 0 \quad (2)$$

thus the force R would be equal to

$$R = \frac{F}{\sin\theta} \tag{3}$$

Since the net moment on pivot A is zero, the moments produced by forces f_u (force exerted by the upper jaw) and R are equal

$$f_u z = Ra \tag{4}$$

in which, z is distance between pivot A and the place contacting tissue on the upper jaw and a is distance between pivot A and B.

Finally substituting (3) into (4) gives

$$f_u = \frac{a}{z}\frac{F}{\sin\theta} \tag{5}$$

Using same method the force exerted by lower jaw yields

$$f_l = \frac{-c}{d}(R - f_u)\cos\theta \tag{6}$$

where c and d are the distance between pivot A and the end of the lower rod and the distance between the point contacting the tissue on the lower rod, respectively.

Therefore, given F, the applied force to the upper rod and x, the position of the upper rod it is possible to determine the exact forces exerted on the tissue. The applied force, F, can be written as the subtraction of f_1, tension of the lower set of SMA wires, and f_2, the tension of the upper set.

2.2. Sensors

Information about applied force and the angular position of the jaws has been achieved using two types of sensors.

2.2.1. Force Measuring Sensors

In order to measure the applied force, two load cells were used at the end of the each set of SMA wires, as shown in Figure 2. Placing the sensors at the end of the wires, avoids any hardware additions to the tool tip, resulting in a smaller tool and thus a better operation performance. The output voltages of load cells are filtered and amplified using two instrumentation amplifiers.

2.2.2. Position Sensors

The position of the upper rod of the grasper can be found by placing a displacement sensor at the end of the upper rod.

3. SYSTEM MODELING AND CONTROL

The ability to place sensors in order to measure the exact applied force on the tissue is one of the advantages of the proposed antagonistic configuration. As discussed before, having feedback of the applied force is essential to prevent the damages caused by applying excessive amount of force on the tissue. However, it is obvious that this cannot be achieved without having any force control algorithm to control the exerted force by the grasper. Based on the required behavior of the system, various control methods may be used. However, the first step in designing a controller is to have a model of the system.

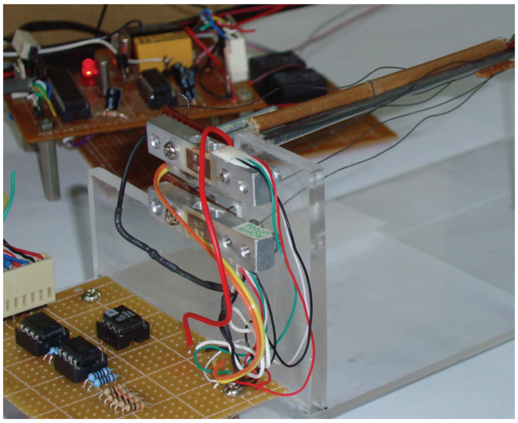

Fig. 2. Placement of force sensors at the end of the SMA wires.

3.1. System Modeling

Biasing a spring with SMA can be replaced by antagonistic configuration to obtain active force control. In this method, two SMA sets apply their forces in opposite directions by the aid of a pulley in which one set of SMA wires is heated while the other is naturally cooled.[9] The resultant force would be

$$Y = (f_1 - f_2) = (\sigma_1 - \sigma_2)A \tag{7}$$

where σ_1 and σ_2 are stresses applied by Set 1 and Set 2 and A is the cross sectional of SMA wires. The time derivative of (7) is

$$\dot{Y} = (\dot{\sigma_1} - \dot{\sigma_2})A \tag{8}$$

According to constitutive equation of SMA, the stress rate ($\dot{\sigma}$) is the function of changes in strain (ϵ), temperature (T) and the mole fraction (ξ):

$$\dot{\sigma} = D\dot{\epsilon} + \theta_T \dot{T} + \Omega\dot{\xi} \tag{9}$$

where D is the average Young's modulus of the alloy, θ_T is the thermal expansion, $\Omega = -D\epsilon_0$ and ϵ_0 is the initial strain. By the process of Joule heating, the Voltage input heat the SMA wire and by considering the natural convection, the heat transfer function can be given by the following equation:[13]

$$mc_p\frac{dT}{dt} = \frac{V^2}{R} - hA(T - T_\infty) \tag{10}$$

The coefficient of h can be written as

$$h = h_0 + h_2 T^2 \tag{11}$$

SMA exists only in Martensite or Austenite phases. Therefore, the heat transition phases could be written as[13]

For heating

$$\dot{\xi} = \frac{\xi^2}{\xi_M}\left\{\exp\left[\frac{T_{f_a} - T}{\sigma_m} + K_a\sigma\right]\left[\frac{\dot{T}}{\sigma_m} - K_a\dot{\sigma}\right]\right\} \tag{12}$$

For cooling

$$\dot{\xi} = \frac{\xi^2}{\xi_a}\left\{\exp\left[\frac{T_{f_m} - T}{\sigma_m} + K_m\sigma\right]\left[\frac{\dot{T}}{\sigma_m} - K_m\dot{\sigma}\right]\right\} \tag{13}$$

The dynamic equations of SMA can be represented in the state space form as follows

$$\dot{\bar{X}} = f(\bar{X},\ u,\ t) \tag{14}$$

where

$$\bar{X} = [Y\ T_1\ \xi_1\ T_2\ \xi_2]^T \tag{15}$$

and u is the input voltage to the SMA wires which will be calculated by the controller. The sign of this voltage determines the active SMA set:

$$\begin{cases} V_1 = 0,\ V_2 = u & \text{if } u > 0 \\ V_1 = -u,\ V_2 = 0 & \text{if } u < 0 \end{cases} \tag{16}$$

Note that since only one SMA set is active at a time, three states will only participate in the system modeling. Using the model parameters listed in Table I and by linearization the above equations about an operating point where the strain rate is zero, a linear model in the form of

$$\dot{\bar{X}} = \mathbf{A}\bar{X} + \mathbf{B}u \quad y = \mathbf{C}\bar{X} \tag{17}$$

can be obtained which has three poles at [−1.3794, −2.6898, −218.6699]. This model is very sensitive to the operating point and specially on the temperature which change the places of poles rapidly.

To support this analytical model with experimental results, a second order linear system with transport delay is presented, which has the following transfer function

$$G(s) = \frac{Ke^{-Ls}}{(T_1 s + 1)(T_2 s + 1)} \tag{18}$$

The parameters of this model have been determined as

$$G(s) = \frac{0.9e^{-0.01s}}{(0.3104s + 1)(0.0041s + 1)} \tag{19}$$

which has two poles at [−3.2216, −243.9024].

As it can be seen, these poles are very close to two of the poles calculated from the analytical model, which supports the proposed analytical and linearized model. Since the second order model has been obtained from the actual data, this model has been used for the purpose of controller design.

Table I. Parameters of the SMA.

Parameter	Value
Mass per unit length (m in $kg \cdot m^{-1}$)	$4.54e^{-4}$
Specific heat capacity (c_p in $J \cdot kg^{-1} \cdot K^{-1}$)	320
Resistance per unit length (R in $\Omega \cdot m^{-1}$)	13.0677
Young's Modulus (Austenite) (D_a in $N \cdot m^{-2}$)	$75e^9$
Young's Modulus (Martensite) (D_m in $N \cdot m^{-2}$)	$28e^9$
Thermal Expansion (θ_t in $N \cdot m^{-2} \cdot s^{-1} \cdot K^{-1}$)	$-11e^{-6}$
SMA initial strain (ϵ_i)	0.03090
Heat convection coefficient (h_0 in $J \cdot m^{-2} \cdot s^{-1} \cdot K^{-1}$)	28.552
Heat convection coefficient (h_2 in $J \cdot m^{-2} \cdot s^{-1} \cdot K^{-3}$)	$4.060e^{-4}$
Diameter of wire (in m)	$381e^{-6}$
Length of wire (in m)	0.24
Ambient temperature (T_a in $°C$)	20
Martensite to Austenite Transformation temperature (T_{f_a} in °C)	90
Austenite to Martensite Transformation temperature (T_{f_m} in °C)	42
Spread of temperature around T_{f_a} (σ_a in °C)	6
Spread of temperature around T_{f_m} (σ_m in °C)	4.5

3.2. Force Control Method

Taking advantage of force sensors, results in a closed loop force controller that increases speed and accuracy of grasper to exert the exact desired force. PID controllers have demonstrated good performance in case of fast convergence and set point tracking.[14] Transfer function of a PID controller is

$$C(s) = K_p\left(1 + \frac{1}{T_i s} + T_D s\right) \tag{20}$$

where K_P, T_I and T_D are proportional, integral and derivative parameters and should be calculated with respect to system's model. Using the model achieved for the system, *Zielger-Nichols (ZN)* control method has been used in order to tune the PID parameters. Calculating the *ultimate gain* (K_u) and *ultimate period* (T_u) of the system in it's *ultimate point* yields:

$$K_u = 45.26, \quad T_u = 1 \tag{21}$$

PID parameters in ZN method are calculated using the following formulas:

$$\begin{cases} K_p = K_u r_b \cos\phi_b \\ T_I = \dfrac{T_u}{\pi}\left(\dfrac{1 + \sin\phi_b}{\cos\phi_b}\right) \\ T_D = \dfrac{\alpha T_u}{\pi}\left(1 + \dfrac{\sin\phi_b}{\cos\phi_b}\right) \end{cases} \tag{22}$$

where α determines the overshoot ratio and ϕ_b and r_b are the system's desired operating point according to application requirements. One of the important considerations in selecting these values is the fact that having overshoot in system's response could bring about tissue damages. By selecting $\alpha = 0.05$, $\phi_b = 10°$ and $r_b = 0.38$ the PID parameters would be $K_P = 16.9375$, $T_I = 0.3793$ and $T_D = 0.0187$. By further tuning these values for achieving better performance, the final PID parameters would be $K_P = 10$, $T_I = 0.5$ and $T_D = 0.0266$.

4. DISCUSSION

Several experiments were conducted with the designed forceps. As expected, similar behaviors observed from both the experimental setup and the minimal grasper. However, due to the smaller size of the final minimal grasper, the speed of opening and closing the jaws in two models were different for a constant voltage. By applying 2.5 V/1 A to the SMA wires, the closing speed for first prototype is 5 seconds and 1 second for the minimal grasper.

In order to determine the operating zone of the forceps, the jaws has been kept at 45 degrees in closing stage with an external object. Figure 3 shows forces of SMA wire sets and their resultant force with and without presence of an external object. As it can be seen, until $t = 3$ s, F is about zero. In $t = 3$ s when the object is grasped, the tension in set 1 increases thus the amount of F increases. Another consideration in designing the controller is actuator's saturation. Figure 4 shows the maximum amount of force achievable before reaching saturation point at series of constant angles. As shown in Figure 4 the maximum ahievable force grows as the angle between the jaws increases.

In Figure 5 both simulation and experimental closed-loop force responses to input steps are illustrated. In order to evaluate the

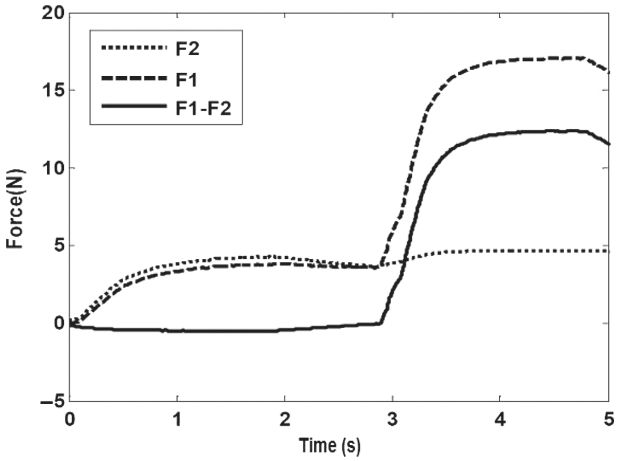

Fig. 3. Experimental results of force sensors. The jaws are held at 45 degrees.

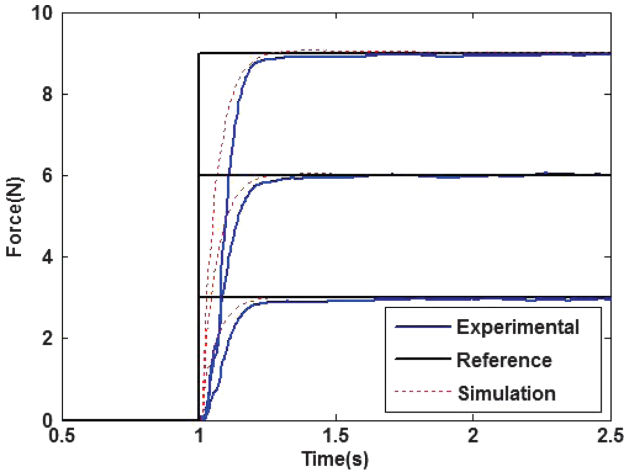

Fig. 5. Simulation and experimental closed loop force step response at closing stage for 3, 6 and 9 N steps.

system's closed-loop performance, the operating zone of the system is divided into three sections and three reference steps with values of 3, 6 and 9 N were applied to the system. These data where obtained when the jaws were being held at 40 degrees. As shown in Figure 5, all three experiments have a similiar transient response. The fluctuation in their steady state responses is due to the nonlinear dynamics of the system. Due to the integrator term of the controller, the response of the system has no seady state errors. According to the results of this experiment, the proposed PID controller has demonstrated a well performance in case of set point tracking and eliminating overshoot in the system's response.

Although color, texture, and visible aspects of the tissue being manipulated can be obtained through the visual feedback available in MIS technology, relying only on these visible aspects could not give a surgeon exact information about the tissue.[5] In other words, without having the tactile information of the tissue it would be extremely difficult, if not impossible, to diagnose and safely handle the grasped tissue. For an advanced control method, information about stress-length ratio of the tissue is necessary. As shown in Figure 3, the feedback of force is dependent on the reaction of tissue to the applied force. Therefore, there

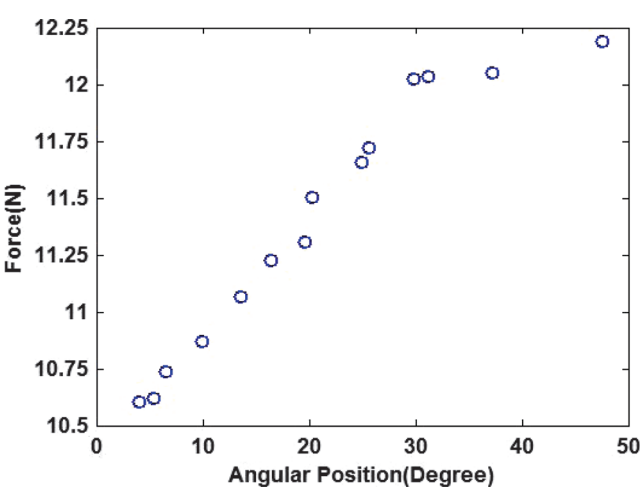

Fig. 4. Maximum exerted force at different angles.

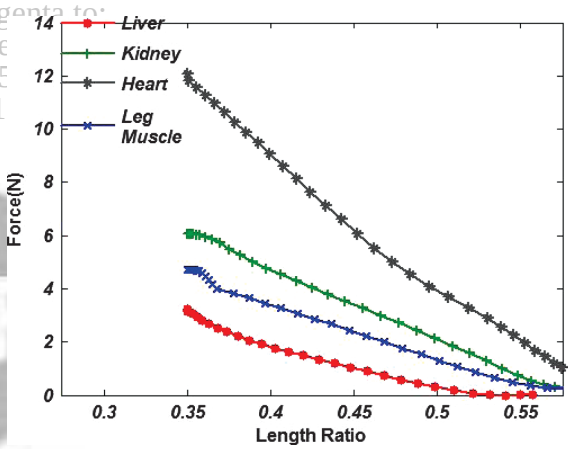

Fig. 6. The experimental stress-length ratio curves for four sheep internal organ tissues.

would be no force feedback until the jaws touch the tissue. During this period the integrator term of controller accumulates the high amount of error and lead the actuator to it's maximum output. To avoid this problem both force and displacement should be considered in the controller design. The relation between force and displacement for different organs could be achieved from the stress-length ratio curves. By having this curve and force feedback information, the controller can predict exactly how much pressure is needed for grasping the tissue in different positions. Figure 6 shows the experimental stress-length ratio curves for four sheep internal organ tissues: Liver, kidney, heart and leg muscle. Since every tissue has a mechanical impedance due to it's own material, this information could also help surgeons for a better identification and diagnose of the grasped tissue. By comparing the force values obtained from this experiment with Figures 3 and 4, it can be seen that the selected operating zone for the system is proper.

5. CONCLUSION

In this paper a new design of forceps with antagonistic shape memory alloy is presented. This SMA configuration helps to

increase speed and place force sensors at the back part of grasper which resolves the problem of lacking force feedback in building minimal forceps. By having force information of system a PID controller is used for accurate tracking of SMA force response. For this forceps, antagonistic SMA configuration exerted great forces between 11–12.75 N with different sets of actuators. Based on measured force by sensors over time a 2nd order linear system with transport delay is determined to find PID parameters. Experimental results for 3 input force steps prove that this PID controller can significantly track setpoint and improve response time. Moreover, using stress-length ratio curves for different organs, this intelligent system could help surgeons to identify the grasped tissue more accurately. As a result of active control that provided by antagonistic configuration, other control schemes such as impedance control methodes can be applied to this system for satisfying different requirements.

References and Notes

1. V. R. C. Kode and M. C. Cavusoglu, Design and characterization of a novel hybrid actuator using shape memory alloy and DC micromotor for minimally invasive surgery applications. *IEEE/ASME Transactions on Mechatronics* 12, 455 **(2007)**.
2. A. R. Lanfranco, A. E. Castellanos, J. P. Desai, and W. C. Meyers, Robotic surgery a current perspective. *Annals of Surgery* 239, 14 **(2004)**.
3. N. Zemiti and G. Morel, A new robot for force control in minimally invasive surgery, *Proc. IEEE/RSJ Int. Conf. Intell. Robot. Syst.* **(2004)**, pp. 3643–3648.
4. R. H. Taylor and D. Stoianovici, Medical robotics in computer integrated surgery. *IEEE Trans. Robot. Autom.* 19, 765 **(2003)**.
5. J. Rosen, B. Hannaford, M. P. MacFarlane, and M. N. Sinanan, Force controlled and teleoperated endoscopic grasper for minimally invasive surgery—Experimental performance evaluation. *IEEE Trans. Biomed. Eng.* 46, 1212 **(1999)**.
6. R. Kornbluh, R. Perline, J. Eckerle, and J. Joseph, Electrostrictive polymer artificial muscle actuators, *Proc. IEEE Int. Conf. Robot. Autom. (ICRA 1998)* **(1998)**, pp. 2147–2154.
7. J. D. W. Madden, N. A. Vandesteeg, P. A. Anquetil, P. G. A. Madden, A. Takshi, R. Z. Pytel, S. R. Lafontaine, P. A. Wieringa, and I. W. Hunter, Artificial muscle technology: Physical principles and naval prospects. *IEEE J. Ocean. Eng.* 29, 706 **(2004)**.
8. M. Moallem and V. A. Tabrizi, Tracking control of an antagonistic shape memory alloy actuator pair. *IEEE Trans. Contr. Syst. Technol.* 17, 184 **(2009)**.
9. V. Gupta, N. P. Reddy, and P. Batur, Forces in surgical tools: Comparison between laparoscopic and surgical forceps. Bridging Disciplines for Biomedicine. *Proceedings of the 18th Annual International Conference of the IEEE*, Engineering in Medicine and Biology Society **(1996)**, Vol. 1, pp. 223–224.
10. P. Puangmali, K. Althoefer, L. D. Seneviratne, D. Murphy, and P. Dasgupta, State-of-the-art in force and tactile sensing for minimally invasive surgery. *IEEE Sensors J.* 8, 371 **(2008)**.
11. C. R. Wagner, N. Stylopoulos, and R. D. Howe, The role of force feedback in surgery: Analysis of blunt dissection, *Haptic interfaces for virtual environment and teleoperator systems, 2002. HAPTICS 2002. Proceedings. 10th Symposium* **(2002)**, pp. 68–74.
12. S. De, J. Rosen, A. Dagan, B. Hannaford, P. Swanson, and M. Sinanan, Assessment of tissue damage due to mechanical stresses. *Intern. J. Robotics Research* 26, 1159 **(2007)**.
13. J. Jayender, R. V. Patel, S. Nikumb, and M. Ostojic, Modeling and control of shape memory alloy actuators. *IEEE Transactions on Control Systems Technology* 16, 279 **(2008)**.
14. Y. H. Tee and R. Featherstone, Accurate force control and motion disturbance rejection for shape memory alloy actuators. *IEEE Intern. Conf. Robotics and Automation,* Rome, Italy **(2007)**, pp. 4454–4459,

Received: 30 May 2011. Revised/Accepted: 22 August 2011.